

used an uncertainty of 10% is assumed. If MLR derived efficiencies are used, then the standard error of each regression coefficient is its uncertainty. For sulfates and nitrates the uncertainty in the relative humidity factor is also included in the extinction to mass uncertainty. Reconstructed extinction for each time period is calculated by

$$B_{i,tot} = \sum_{j=1}^J B_{i,j} \quad (5.8)$$

Reconstructed scattering is the same except that absorption by NO_2 and LAC would not be included in the sum. Rayleigh scattering can also be included by including it in the sum. The uncertainty in the reconstructed extinction for each time period is

$$BU_{i,tot} = \sqrt{\sum_{j=1}^J BU_{i,j}^2} \quad (5.9)$$

where J is the total number of chemical species. The fraction of extinction due to each species for each time period is

$$F_{i,j} = B_{i,j} / B_{i,tot} \quad (5.10)$$

and the uncertainty in these fractions are calculated by

$$FU_{i,j} = \sqrt{\frac{BU_{i,j}^2}{B_{i,tot}^2} + \frac{B_{i,j}^2 BU_{i,tot}^2}{B_{i,tot}^4}} \quad (5.11)$$

The mean extinction for the entire WHITEX study due to each chemical species is calculated by

$$B_{mean,j} = \frac{1}{I} \sum_{i=1}^I B_{i,j} \quad (5.12)$$

where I is the total number of time periods. and the mean reconstructed extinction is

$$B_{mean,tot} = \frac{1}{I} \sum_{i=1}^I B_{i,tot} \quad (5.13)$$

The mean fractions of extinction due to each species were calculated by

$$F_{mean,j} = \frac{B_{mean,j}}{B_{mean,tot}} \quad (5.14)$$

and the uncertainties in the mean fractions are

$$FU_{mean,j} = \sqrt{\frac{BU_{mean,j}^2}{B_{mean,tot}^2} + \frac{B_{mean,j}^2 BU_{mean,tot}^2}{B_{mean,tot}^4}} \quad (5.15)$$

5.2 Preliminary Data Analysis

Before attempting the estimation of light extinction efficiencies and budgets with WHITEX data, some preliminary analyses of the data were performed. These included (1) an investigation of extinction coefficients measured by the transmissometer compared to scattering coefficients measured by the integrating nephelometer for the full range of relative humidity conditions; and (2)

comparisons of the results of several analyses using the extinction and scattering coefficients and particulate matter concentrations for separate carbon and nitrate data sets. These were used to examine whether use of light extinction data could help resolve the discrepancies between collocated measurements of carbon and nitrate and perhaps illuminate which data sets would be more appropriate to use in subsequent analyses, including estimation of extinction efficiencies and budgets. Refer to Chapter 3 for more discussion of the carbon and nitrate measurements.

5.2.1 Optical Data and Relative Humidity Effects

Historically, most short term and many long term visibility research programs have relied on the integrating nephelometer as the instrument of choice for measuring atmospheric aerosol scattering. Atmospheric extinction was then approximated by estimating the absorption coefficient. Atmospheric absorption is usually determined using the laser integrating plate method (LIPM) or by measuring elemental carbon and assuming a light absorption efficiency. Given the large discrepancies found in this and other studies between elemental carbon measurements and between elemental carbon derived absorption and LIPM, determinations of extinction by these methods are approximate at best.

Fortunately, Page, Canyonlands, and Hopi Point, were each equipped with both a nephelometer and a transmissometer, which measures extinction directly. This allowed intercomparison of the scattering coefficients measured by the nephelometer (b_{scat}) to the extinction coefficients measured by the transmissometer (b_{ext}). Relative humidity (RH) was also monitored at each of these sites. Time traces of these data, as well as the differences between b_{ext} and b_{scat} and the ratios of b_{ext}/b_{scat} are shown in Figures 5.2, 5.3, and 5.4. Note that the largest extinction coefficients occurring during WHITEX were measured at Page during Feb. 11 - 13 (Julian days 42 - 44) when the relative humidity remained above 60 percent for several days.

At Hopi Point and Canyonlands, transmissometer data are often missing when the relative humidity is high. This is a result of the altitudes of these sites (7100 and 5925 feet above mean sea level, respectively) which frequently causes the sight paths to be obscured by clouds on high RH days. The elevation at Page (4180 feet) is apparently low enough so that this did not occur as frequently.

Scatter plots of the ratios of b_{ext}/b_{scat} as a function of relative humidity are shown in Figures 5.5, 5.6, and 5.7 for the three sites. The mean ratios are near unity (1.09, 1.14, and 1.03 for Page, Canyonlands, and Hopi Point respectively) when the relative humidity is below 60 percent. As discussed above, there are few transmissometer data at Hopi Point and Canyonlands when the relative humidity is higher than this. However, at Page, it can be seen that the ratio increases dramatically as the relative humidity increases from 70 to near 100 percent. It is known that unmodified nephelometers tend to heat air as it passes through the sampling chamber and, as such, "dry" hygroscopic aerosols, thus reducing their scattering efficiency.^{6, 8} Drying the aerosol in the nephelometers used during the WHITEX study appears to cause underestimation of atmospheric scattering by a factor of nearly 3 during high (greater than 90 percent) relative humidity conditions.

Inspection of the time plots for Canyonlands reveals an apparent offset problem between the transmissometer and nephelometer after January 16. The offset is approximately 0.003-0.004 Km^{-1} . To correct for this, in all following analyses, 0.0035 Km^{-1} was subtracted from all b_{ext} data after January 16 at Canyonlands. Tables 5.10, 5.11, and 5.12 include the means and other statistics for the optical data. The statistics for Canyonlands include the 0.0035 Km^{-1} correction. Note that mean b_{scat} is greater than mean b_{ext} at Hopi Point. This is probably due to the time periods with high RH when b_{ext} was missing because the transmissometer site path was obscured by clouds but b_{scat} data existed. During many of these time periods, the measured scattering was relatively high.

PAGE

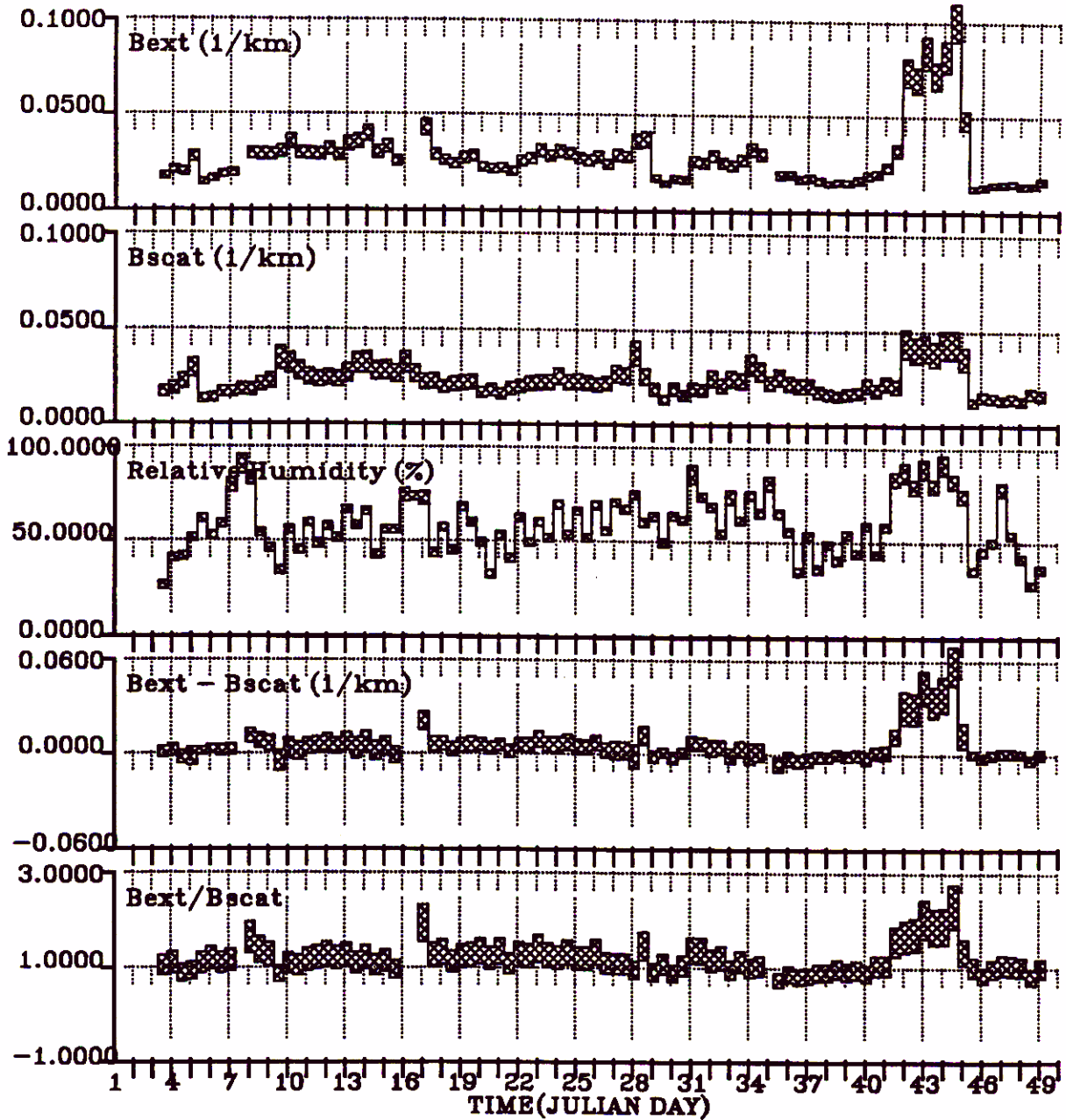


Figure 5.2: Time traces of optical data and relative humidity at Page

CANYONLANDS

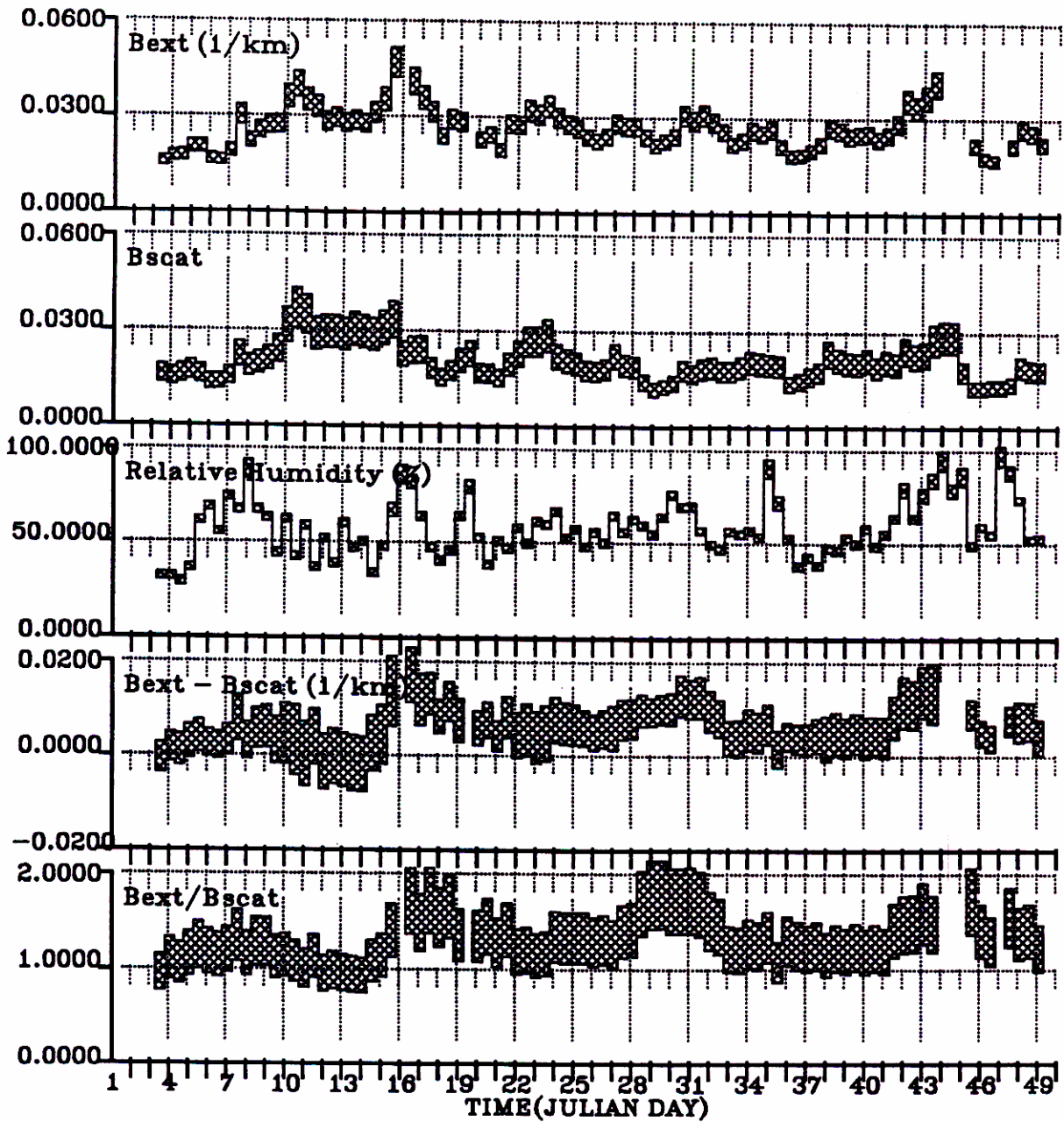


Figure 5.3: Time traces of optical data and relative humidity at Canyonlands.

HOPI POINT

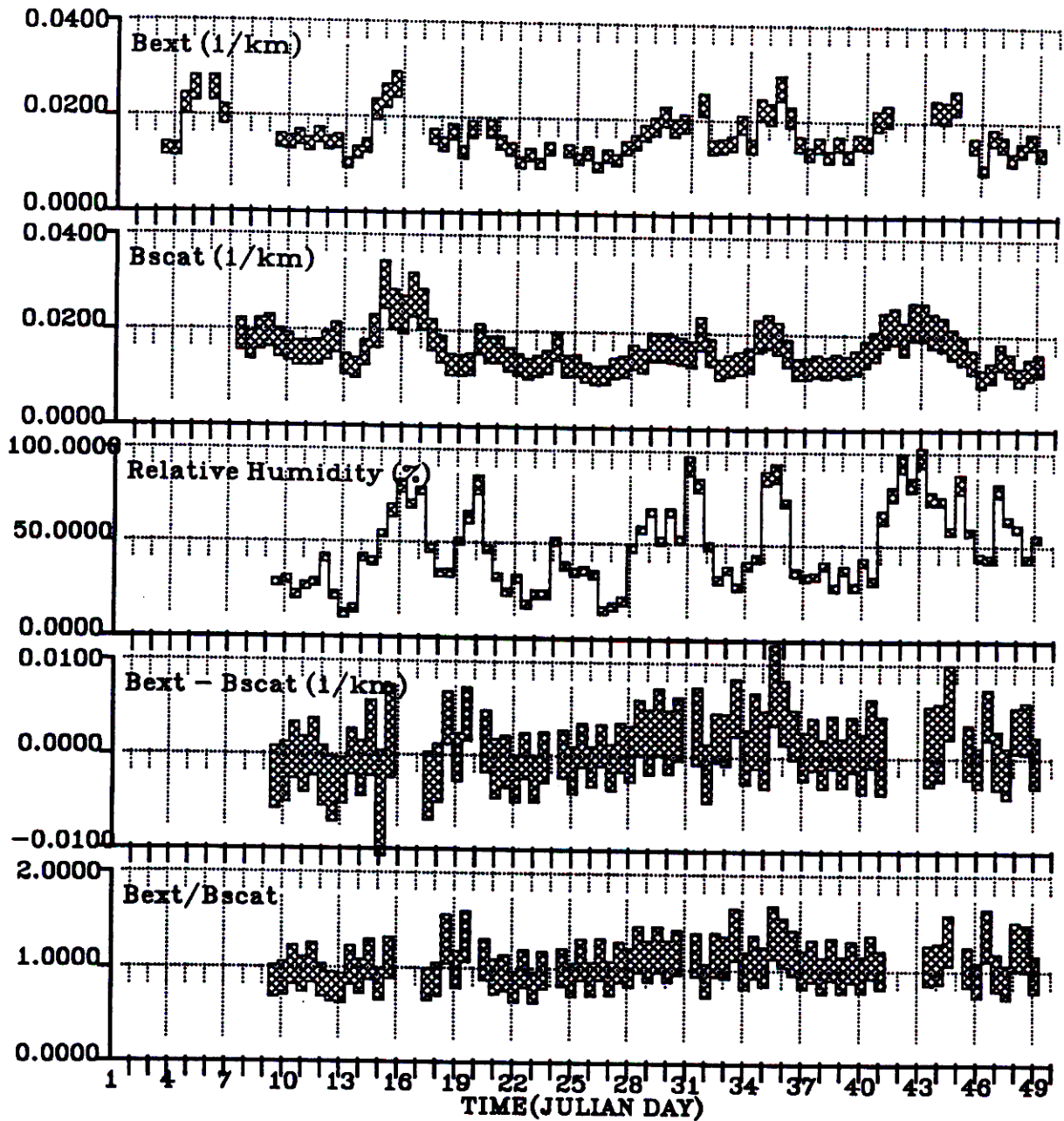


Figure 5.4: Time traces of optical data and relative humidity at Hopi Point.

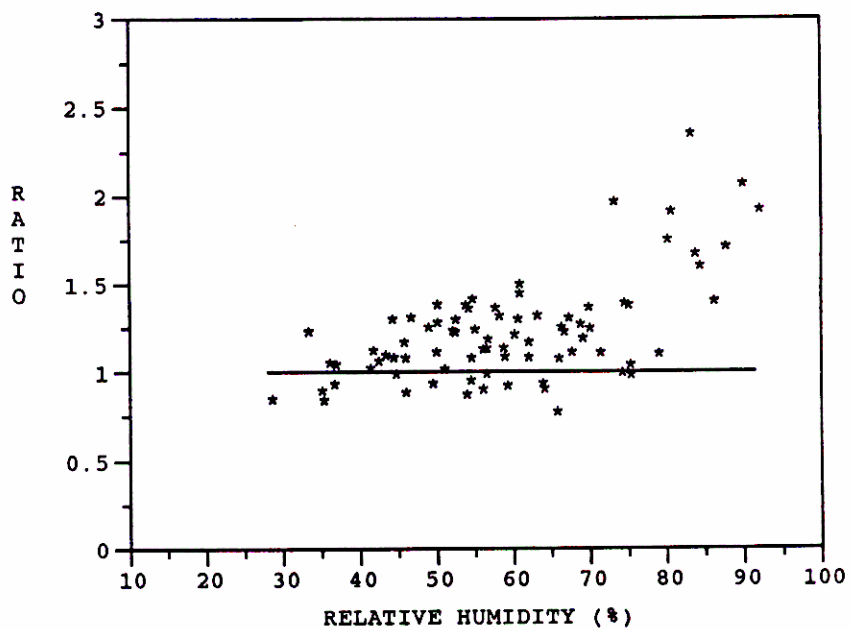


Figure 5.5: Ratio of b_{ext}/b_{scat} as a function of relative humidity for Page.

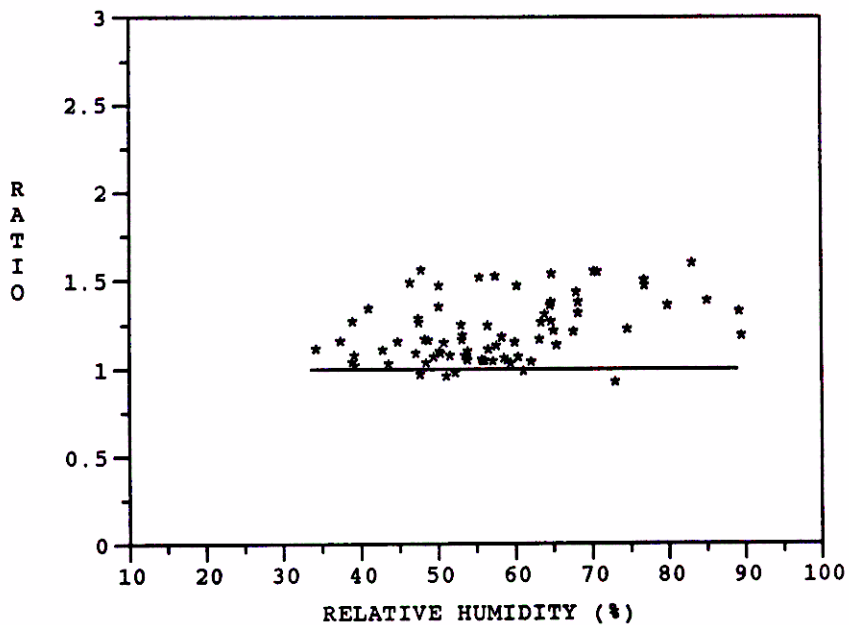


Figure 5.6: Ratio of b_{ext}/b_{scat} as a function of relative humidity for Canyonlands.

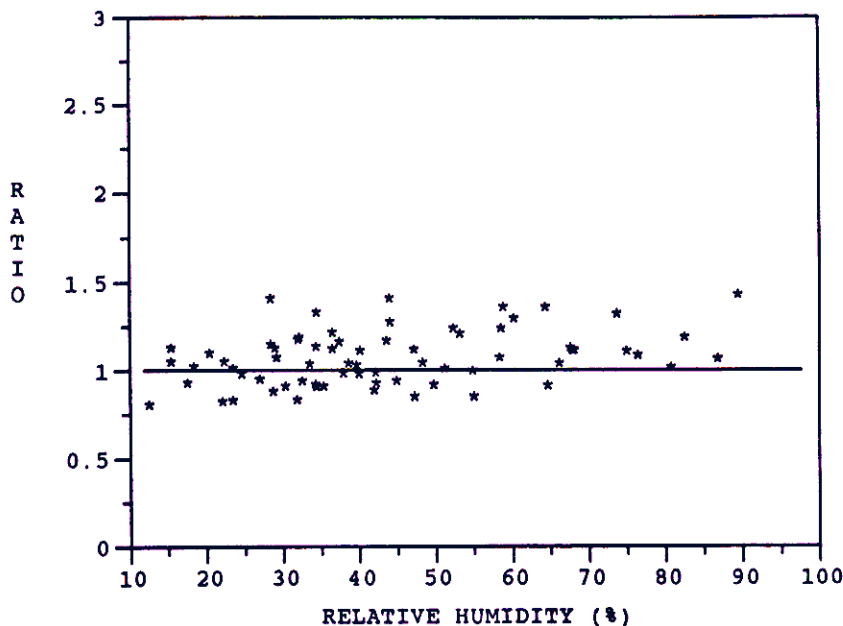


Figure 5.7: Ratio of b_{ext}/b_{scat} as a function of relative humidity for Hopi Point.

To confirm this the means of b_{ext} and b_{scat} only for time periods when both measurements were nonmissing were also calculated. The mean b_{ext} for these 69 time periods was 0.0161 Km^{-1} and the mean b_{scat} was 0.0154 . No corrections were made to this data set.

5.2.2 Examination of Carbon Data

At Page and Hopi Point measurements of carbonaceous material were made by both IMPROVE and SCISAS samplers. Data from the IMPROVE samplers were analysed using the thermal optical reflectance (TOR) method. Data from SCISAS samplers were analysed by the thermal MnO_2 oxidation (TMO) method. As discussed in Appendix 3D, the organic carbon concentrations from the two methods agree fairly well at Page. At Hopi Point, only 4 of the 84 concentrations of TOR organic carbon are above the minimum detection limit and the 4 concentrations higher than the detection limit do not agree well with the TMO organic carbon concentrations for the same time periods. The elemental or "light absorbing" carbon, while correlating well at both sites, differ by a factor of approximately 5 with the TOR concentrations being greater. Scatter plots of these data are in the Appendix 3D. Correlation matrices are shown in Tables 5.13 and 5.14.

To determine whether TOR or TMO data are more appropriate for use in the extinction budget analyses, three tests of the data were performed. These included 1) calculating reconstructed extinction with both data sets, to see which better reproduced measured light extinction; 2) MLR analyses regressing TOR and TMO carbon against b_{ext} to see if realistic absorption efficiencies would result; and 3) estimating the expected mean light absorbing carbon (LAC) concentrations for each site based on the optical measurements.

Because so many of the TOR organic carbon concentrations are below detection limit at Hopi Point, all analyses using TOR carbon for that site were done two ways: (1) TOR organics less than minimum detection limit were set to the detection limit (the "maximum organics" case) and (2)

Table 5.10: Statistics for the 12-hour averaged optical data at Page (Km^{-1}). The low relative humidity subgroup is defined as $\text{RH} < 60\%$.

Humidity Subgroup	Variable	Page				Number of Cases
		Mean	Standard Deviation	Minimum	Maximum	
All	b_{ext}	.0292	.0166	.0126	.1000	80
Low	b_{ext}	.0228	.0067	.0126	.0356	45
All	b_{scat}	.0235	.0074	.0123	.0437	84
Low	b_{scat}	.0208	.0052	.0123	.0347	45
All	b_{ext}/b_{scat}	1.20	0.30	0.75	2.32	80
Low	b_{ext}/b_{scat}	1.09	0.16	0.81	1.39	45
All	$b_{ext}-b_{scat}$.0058	.0107	-.0064	.0570	80
Low	$b_{ext}-b_{scat}$.0020	.0034	-.0046	.0081	45
All	RH(%)	59.7	15.0	28.0	91.4	84
Low	RH(%)	48.3	8.1	28.0	59.6	45

Table 5.11: Statistics for the 12-hour averaged optical data at Canyonlands (Km^{-1}). The low relative humidity subgroup is defined as $\text{RH} < 60\%$.

Humidity Subgroup	Variable	Canyonlands				Number of Cases
		Mean	Standard Deviation	Minimum	Maximum	
All	b_{ext}	.0247	.0064	.0134	.0470	78
Low	b_{ext}	.0232	.0058	.0134	.0400	51
All	b_{scat}	.0211	.0056	.0119	.0369	84
Low	b_{scat}	.0207	.0060	.0119	.0369	51
All	b_{ext}/b_{scat}	1.19	0.17	0.90	1.57	78
Low	b_{ext}/b_{scat}	1.14	0.15	0.93	1.53	51
All	$b_{ext}-b_{scat}$.0036	.0035	-.0020	.0137	78
Low	$b_{ext}-b_{scat}$.0024	.0026	-.0020	.0097	51
All	RH(%)	59.5	14.5	33.7	97.4	84
Low	RH(%)	50.0	6.7	33.7	59.9	51

Table 5.12: Statistics for the 12-hour averaged optical data at Hopi Point (Km^{-1}). The low relative humidity subgroup is defined as $\text{RH} < 60\%$.

Hopi Point						
Humidity Subgroup	Variable	Mean	Standard Deviation	Minimum	Maximum	Number of Cases
All	b_{ext}	.0161	.0041	.0099	.0270	69
Low	b_{ext}	.0150	.0033	.0099	.0244	56
All	b_{scat}	.0163	.0038	.0109	.0296	84
Low	b_{scat}	.0150	.0030	.0109	.0296	61
All	b_{ext}/b_{scat}	1.05	0.16	0.78	1.40	69
Low	b_{ext}/b_{scat}	1.03	0.15	0.78	1.38	56
All	$b_{ext}-b_{scat}$.0007	.0024	-.0052	.0078	69
Low	$b_{ext}-b_{scat}$.0004	.0023	-.0052	.0061	56
All	RH(%)	48.3	22.2	11.9	97.6	80
Low	RH(%)	36.4	12.3	11.9	59.6	57

Table 5.13: Correlation matrix for carbonaceous material at Page.

	TOR		TMO	
	organic carbon	TOR abs. C	organic carbon	TMO abs. C
TOR organic	1.000	0.714	0.678	0.516
TOR abs. C	0.714	1.000	0.853	0.743
TMO organic	0.678	0.853	1.000	0.863
TMO abs. C	0.516	0.743	0.863	1.000

Table 5.14: Correlation matrix for carbonaceous material at Hopi Point.

	Max	Min	TMO		
	TOR organic carbon	TOR organic carbon	TOR abs. C	organic carbon	TMO abs. C
Max TOR organic	1.000	0.927	0.533	0.109	0.108
Min TOR organic	0.927	1.000	0.471	0.094	0.105
TOR abs. C	0.553	0.471	1.000	0.503	0.418
TMO organic	0.109	0.094	0.503	1.000	0.809
TMO abs. C	0.108	0.105	0.418	0.809	1.000

TOR organics less than the minimum detection limit were set to zero (the "minimum organics" case).

Reconstructed Extinction

The first test of the LAC concentrations was to calculate reconstructed light extinction with the consensus literature scattering and absorption efficiencies shown in Table 5.9. The analyses were done using both the Trijonis and Pitchford¹³ and the modified Tang¹² scattering efficiencies for nitrates and sulfates and for both the TOR and TMO carbon concentrations. Results were then compared to the measured b_{ext} . Absorption due to NO_2 was included in the reconstructed extinction when data were available, otherwise it was set to zero. There are no NO_2 data at Hopi Point and NO_2 data at Page are missing for most high extinction days. This could cause reconstructed extinction to be as much as 4% too low at Page for the days when NO_2 was missing. The underestimation would be less at Hopi Point (perhaps 1-3%) since NO_2 concentrations there are probably lower relative to the particulate concentrations than they are at Page.

Results for are shown in Figures 5.8, 5.9, 5.10, 5.11, 5.12, 5.13, 5.14, 5.15, 5.16, and 5.17. They show that at Page, the reconstructed extinction is closer to the measured when TMO carbon is used. The TOR concentrations cause the reconstructed extinction to be too high. However, at Hopi Point, the reverse is true. The TOR carbon concentrations result in reconstructed extinction which is closer to measured. TMO carbon causes reconstructed extinction to be too low. Another observation which can be made is that the $1/(1-\text{RH})$ correction for sulfates and nitrates is too high. Use of the modified Tang curves eliminates the problem of overestimating the reconstructed extinction during high RH time periods.

Regression Analysis

A second preliminary test of the carbon data was performed by subjecting the data to multiple linear regression (MLR) analyses with b_{ext} as the dependent variable and the chemical species concentrations as the independent variables. The resulting regression coefficients are estimates of the scattering and absorption efficiencies of each species. Use of the absorbing carbon data which are most suitable should then result in an absorption efficiency which is closer to the consensus literature value ($9-12 \text{ m}^2/\text{g}$).

Three different regressions were done for each site (Hopi Point, Page, and data from the sites combined) and each set of absorbing carbon data (TMO and TOR). Regressions were done using two different sets of independent variables. They were (1) absorbing carbon, other fine mass, and coarse mass for cases when the relative humidity was less than 60 percent and (2) absorbing carbon, sulfates, nitrates, organics, soil, and coarse mass for both the low relative humidity subgroup and for all data. Sulfates and nitrates were corrected for relative humidity effects using the modified Tang curves when data at all humidities were used.

The absorption efficiencies predicted for absorbing carbon by each of these MLR analyses are shown in Table 5.15. At Page, all of the MLR coefficients for TOR absorbing carbon were insignificant ($t > .05$). Use of TMO absorbing carbon at Page resulted in significant, but negative efficiencies with large magnitudes for two cases and an insignificant coefficient for the third case. Results for Hopi Point, when TOR carbon was used, were in the range of expected values, ranging from 5.6 to $10.6 \text{ m}^2/\text{g}$, although the case with the lowest coefficient was insignificant. When TMO carbon was used for Hopi Point, all resulting coefficients were insignificant. Regressions using data from Page and Hopi Point combined, and for Page, Hopi Point, and Canyonlands combined resulted

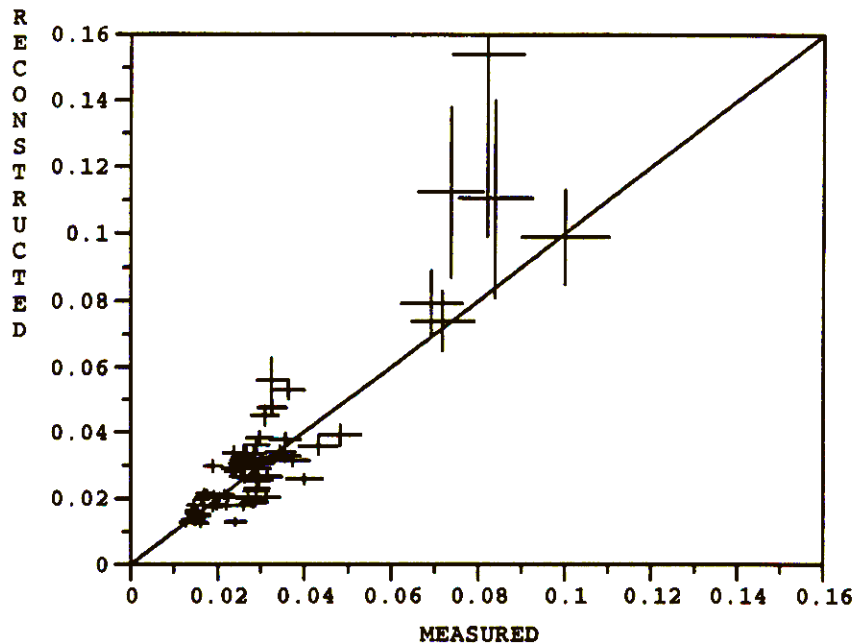


Figure 5.8: Scatter plot of measured extinction vs reconstructed extinction for Page using TMO carbon. Sulfate and nitrate scattering efficiencies are both $2.55/(1-RH)$.

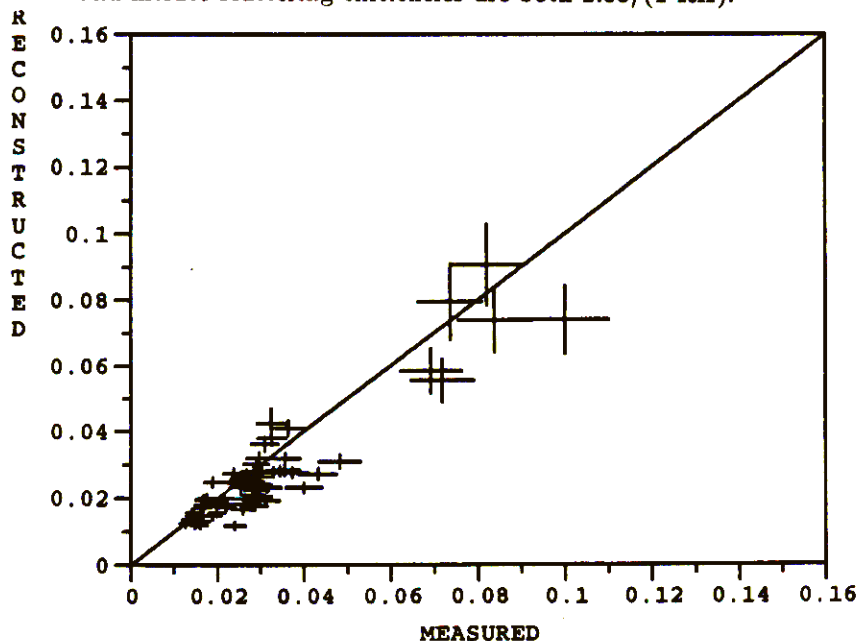


Figure 5.9: Scatter plot of measured extinction vs reconstructed extinction for Page using TMO carbon. Sulfate scattering efficiency is $2.55 \times f_s(RH)$. Nitrate scattering efficiency is $1.1 \times f_n(RH)$.

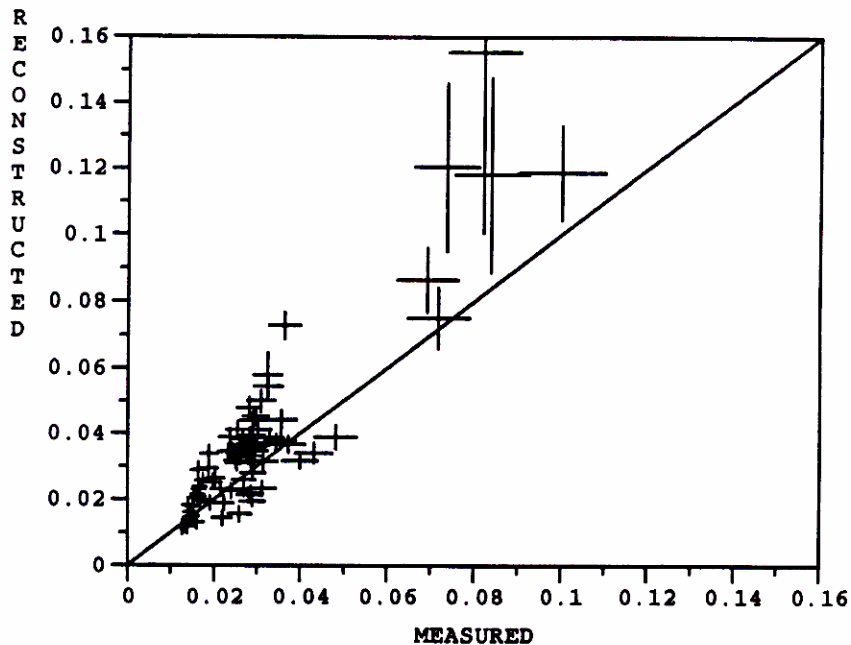


Figure 5.10: Scatter plot of measured extinction vs reconstructed extinction for Page using TOR carbon. Sulfate and nitrate scattering efficiencies are both $2.55/(1-RH)$.

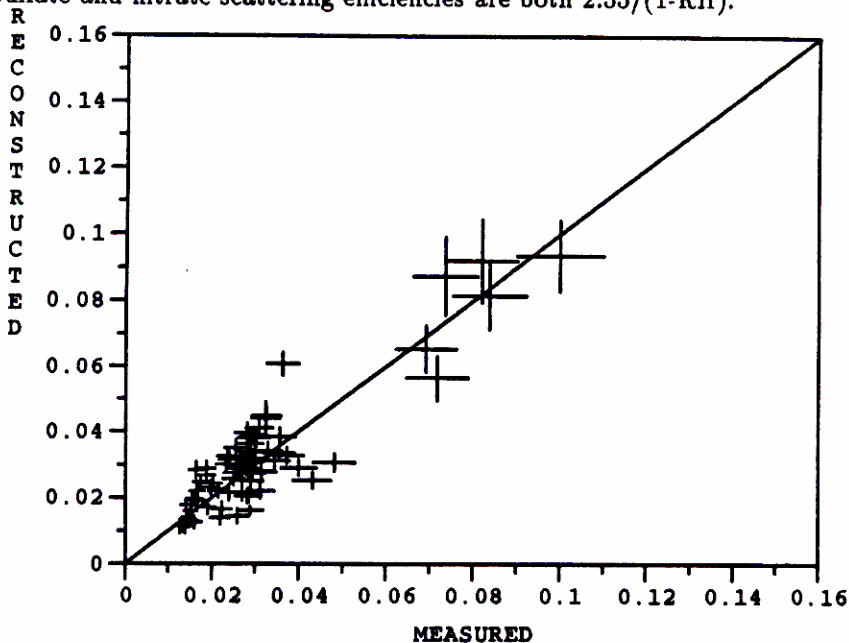


Figure 5.11: Scatter plot of measured extinction vs reconstructed extinction for Page using TOR carbon. Sulfate scattering efficiency is $2.55 \times f_s(RH)$. Nitrate scattering efficiency is $1.1 \times f_n(RH)$.

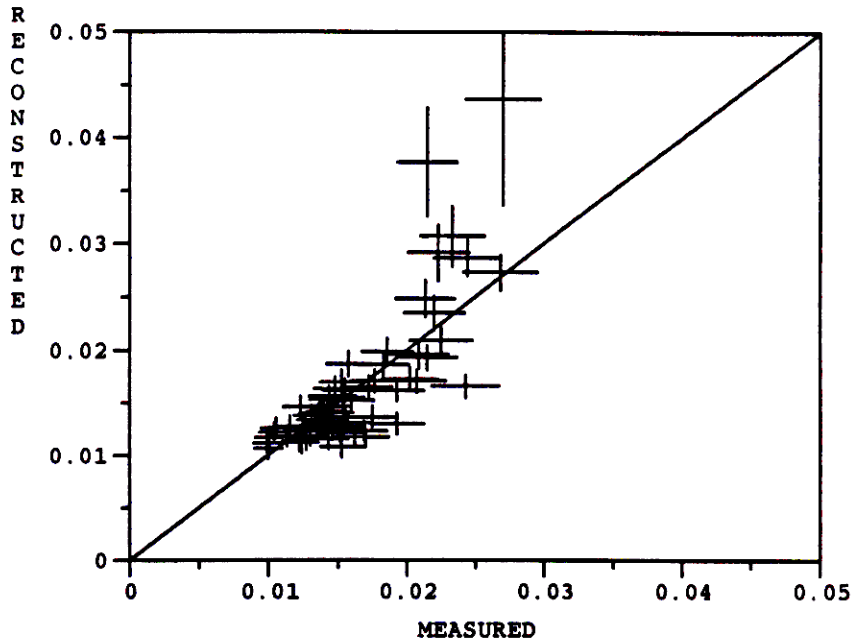


Figure 5.12: Scatter plot of measured extinction vs reconstructed extinction for Hopi Point using TMO carbon. Sulfate and nitrate scattering efficiencies are both $2.55/(1-RH)$.

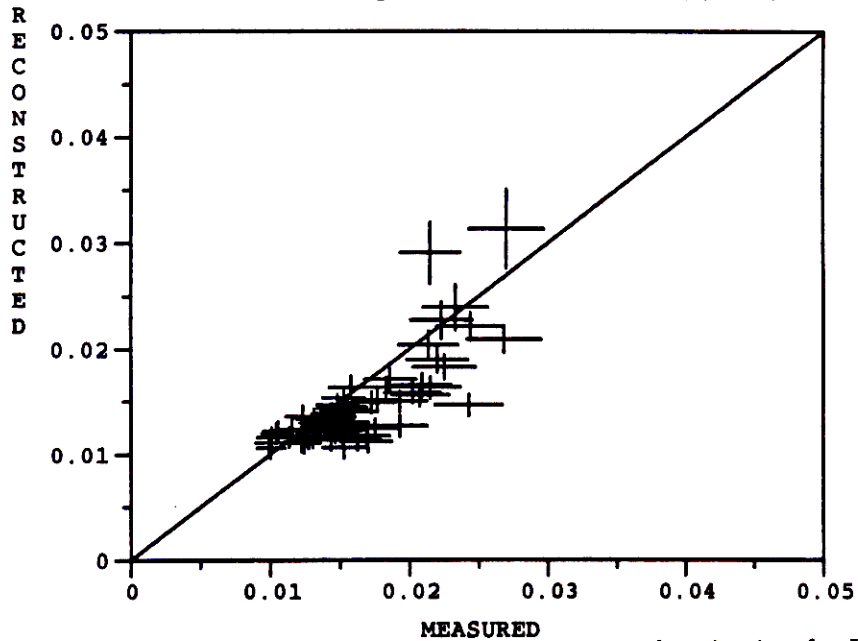


Figure 5.13: Scatter plot of measured extinction vs reconstructed extinction for Hopi Point using TMO carbon. Sulfate scattering efficiency is $2.55 \times f_s(RH)$. Nitrate scattering efficiency is $1.1 \times f_n(RH)$.

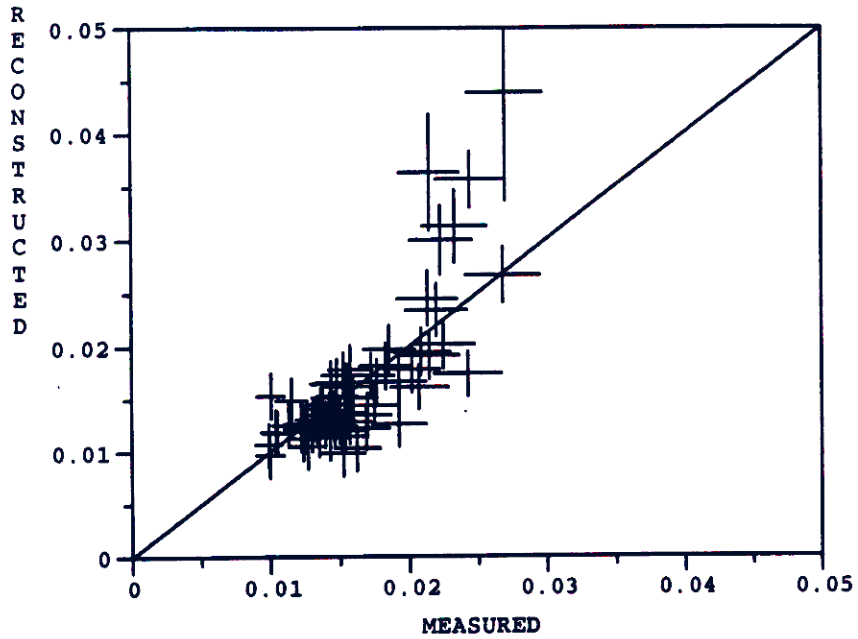


Figure 5.14: Scatter plot of measured extinction vs reconstructed extinction for Hopi Point using minimum TOR carbon. Sulfate and nitrate scattering efficiencies are both $2.55/(1-RH)$.

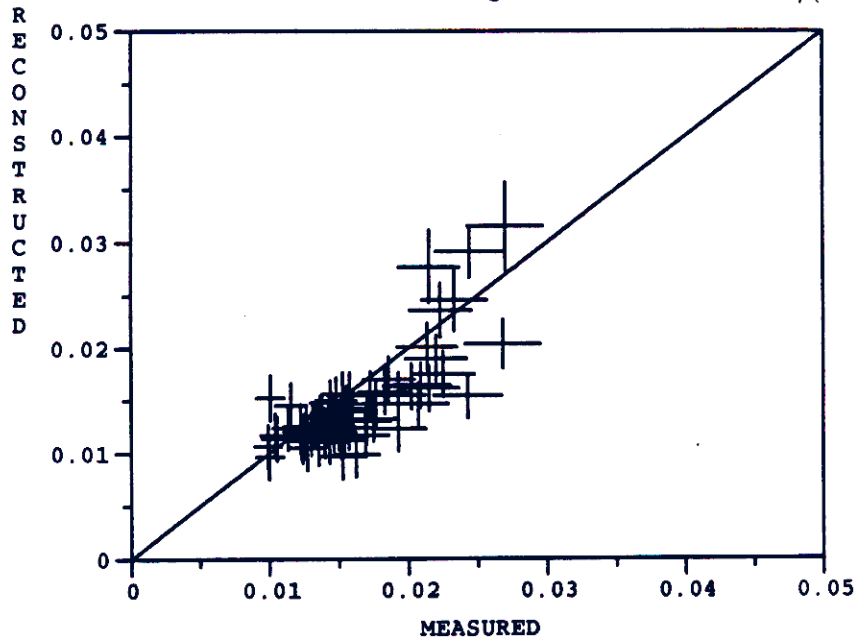


Figure 5.15: Scatter plot of measured extinction vs reconstructed extinction for Hopi Point using minimum TOR carbon. Sulfate scattering efficiency is $2.55 \times f_s(RH)$. Nitrate scattering efficiency is $1.1 \times f_n(RH)$.

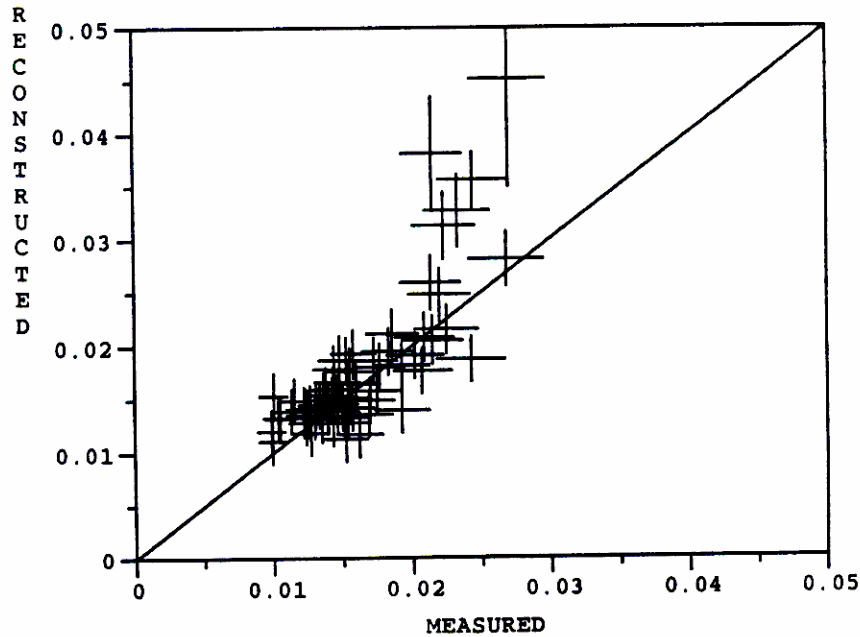


Figure 5.16: Scatter plot of measured extinction vs reconstructed extinction for Hopi Point using maximum TOR carbon. Sulfate and nitrate scattering efficiencies are both $2.55/(1-RH)$.

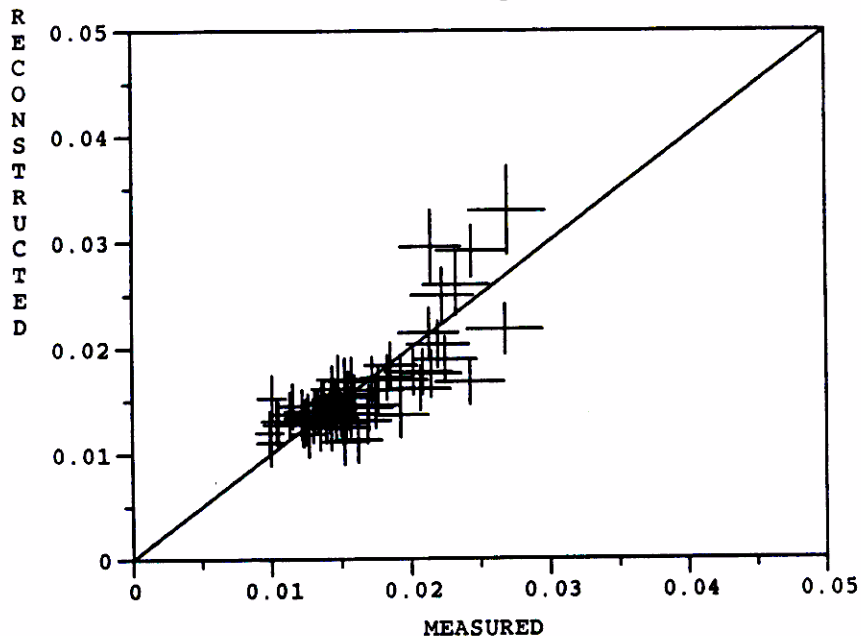


Figure 5.17: Scatter plot of measured extinction vs reconstructed extinction for Hopi Point using maximum TOR carbon. Sulfate scattering efficiency is $2.55 \times f_s(RH)$. Nitrate scattering efficiency is $1.1 \times f_n(RH)$.

Table 5.15: Summary of multiple linear regression analyses using TOR and TMO Carbon. Results are the predicted light absorption efficiencies for absorbing carbon \pm the standard error in m^2/g . The dependent variable for all analyses was b_{ext} . Low RH refers to $RH < 60\%$.

Site	Independent Variables	RH Subgroup	Results for Minimum TOR Carbon	Results for Maximum TOR Carbon	Results for TMO Carbon
Page	all species	All	*-0.0 \pm 4.1		-89.7 \pm 35.8
Page	all species	Low	*-2.3 \pm 5.6		-121.6 \pm 36.9
Page	abs. C, other, coarse	Low	*4.6 \pm 4.0		*-12.5 \pm 30.1
Hopi	all species	All	8.4 \pm 3.5	8.6 \pm 3.4	*-36.4 \pm 53.6
Hopi	all species	Low	*5.6 \pm 4.2	*5.8 \pm 4.2	*-11.3 \pm 64.4
Hopi	abs C., other, coarse	Low	10.6 \pm 4.6	10.8 \pm 4.8	*67.9 \pm 57.6
Both	abs. C., other, coarse	Low	11.1 \pm 2.5	11.1 \pm 2.5	55.4 \pm 16.3
All	abs C., other	Low	7.3 \pm 2.5	7.3 \pm 2.4	No data at Cany

*These values are statistically insignificant ($t > 0.05$).

in significant and reasonable coefficients for TOR carbon, and a larger than reasonable coefficient for TMO carbon.

The negative results may be physically reasonable because the presence of light absorbing carbon can reduce light extinction due to chemical or physical interactions between the carbon and other aerosol constituents.⁹ One scenario in which additional carbon could reduce light scattering is by changing the particle size distribution. If the aerosol particles consist of insoluble carbonaceous cores with hygroscopic ammonium sulfate coatings then the particles would tend to be larger if the carbon concentration was lower. Assuming the same ammonium sulfate concentration, more carbon means there are more nuclei available, thus the aerosols would be smaller and perhaps scatter less efficiently.

Since the regression coefficients for TOR were more reasonable than the results obtained using TMO carbon, this analysis indicates that the TOR values are more appropriate for use in visibility analyses and that the TMO derived concentrations are underestimates of the light absorbing carbon.

Extinction Derived Absorbing Carbon

One final analysis was done to investigate which of the light absorbing carbon data sets is most suitable. The differences between b_{ext} and b_{scat} when the relative humidity is low should be primarily due to atmospheric absorption. Then the expected absorbing carbon concentrations can be approximated by

$$Absorbing\ Carbon = (b_{ext} - b_{scat})/9.0 \quad RH < 60 \quad (5.16)$$

where 9.0 is the expected absorption efficiency in m^2/g . Since b_{scat} as measured by the nephelometer does not include all of the large particle scattering and hence somewhat underestimates the total scattering, this equation would be expected to overestimate the absorbing carbon concentrations. Another assumption is that all of the absorption is due to carbon. If this is not true, then the calculation would overestimate light absorbing carbon by an additional, though probably very small, amount.¹³

At Page, the calculation yielded a mean extinction-derived absorbing carbon (with negative values included) of $0.270 \mu g/m^3$. The means of the TOR and TMO absorbing carbon data for the

same time periods are 0.441 and 0.090 $\mu\text{g}/\text{m}^3$, respectively. At Hopi Point, the extinction derived concentration was 0.039 $\mu\text{g}/\text{m}^3$, while means of TOR and TMO absorbing carbon are 0.137 and 0.025 $\mu\text{g}/\text{m}^3$, respectively. Based on this analysis, it appears that the TMO derived absorbing carbon measurements, on average, are too low and TOR concentrations are too high.

Recommendations

Evidence from the three preliminary analyses is inconclusive. The reconstructed extinction analysis shows that using TOR concentrations gives more reasonable results at Hopi Point, but TMO gives better results at Page. Use of multiple linear regression analysis to estimate the absorption efficiency indicates that TOR carbon is more reasonable. And finally, calculation of the mean extinction derived light absorbing carbon shows that TMO carbon is probably too low, while TOR is too high.

Though the preliminary analyses are inconclusive, it was decided that when calculating the WHITEX extinction budgets, TOR carbon concentrations would be used rather than TMO. Because there are so many TOR organic carbon concentrations which are less than the minimum detection limit at Hopi Point, all analyses for that site were done with both "maximum organics" (organics less than the minimum detection limit set to the detection limit) and "minimum organics" (organics less than the detection limit set to zero).

5.3 Light Extinction Budget By Extinction Type

For each of the sites for which there are adequate data, light extinction is apportioned into absorption by gases, absorption by particles, scattering due to gases, and scattering by fine and coarse particles.

There are no coarse mass data for Canyonlands and gaseous NO_2 concentrations exist only for Page. Consequently, a full extinction budget by type can be explicitly calculated only for Page. A budget by type for all constituents except absorption by NO_2 is possible for Hopi Point. Since NO_2 concentrations were low at Page and probably lower at all other WHITEX sites, this is not a serious obstacle. Coarse mass scattering as well as gaseous absorption must be estimated for Canyonlands. Time plots of all the relevant particulate and gaseous data for Page, Canyonlands, and Hopi Point are shown in Figures 5.18, 5.19, and 5.20. Statistics for the same data are shown in Tables 5.16, 5.17, and 5.18.

To generate the extinction budgets by type for each site, the mean extinction coefficients for each extinction type were estimated independently. The details of these calculations are discussed in the following subsections. Not unexpectedly, the sums of the components do not exactly equal the means of the measured extinction coefficients. The fractions of light extinction allocated to each component are determined by dividing the estimated mean coefficient for each type by the sum of the means for all types. Rayleigh scattering is included in the total. Table 5.19 summarizes the extinction budgets by type for each of the three sites. The budgets for the three sites are also illustrated by the pie charts shown in Figure 5.3.

5.3.1 Scattering by gases (Rayleigh Scattering)

Scattering of light by air molecules is referred to as Rayleigh scattering. The amount of Rayleigh scattering or "clean" air scattering is dependent on the wavelength of the light and on the density of air molecules. Assuming that air density depends mostly on altitude, the average Rayleigh